Liquid crystalline phase in ethanol suspension of anisometric 4-cyano-4-n-hexylbiphenyl microcrystals: Witnessed by dielectric spectroscopy

Zhen Chen and Ryusuke Nozaki[a)]
Department of Physics, Faculty of Science, Hokkaido University, Sapporo 060-0810, Japan

(Received 14 April 2009; accepted 21 April 2010; published online 26 May 2010)

The suspensions of 4-cyano-4-n-hexylbiphenyl (6CB) anisometric microcrystal were obtained by quenching homogeneous 6CB/ethanol mixtures with different 6CB concentrations. Such suspensions were strongly suggested from the differential scanning calorimetry examinations and the image observations of the samples during the quench and heating processes. The crystallization process for the mixtures with higher 6CB concentration looked like the isotropic-nematic phase transition of bulk liquid crystal. Dielectric measurement was carried out on the mixtures during the heating process after quench. Distinct dielectric relaxation was observed in the frequency range between kHz and 100 kHz, which exhibited obvious dependence on temperature and 6CB concentration. Curve fitting on the complex conductivity spectra indicates that three Debye type relaxations exist in this narrow frequency range. Based on the dependences of relaxation parameters on temperature and 6CB concentration, the possible relaxation mechanisms and the phase conformation of the mixtures were discussed. It was concluded that the relaxations, from high to low relaxation frequency, originate from the Maxwell–Wagner polarization, the rotation of 6CB microcrystal around its long axis, and the reorientation of 6CB microcrystal around its short axis, respectively. It was also confirmed that the quenched 6CB/ethanol mixtures show isotropic-nematic phase transition with the increase of 6CB concentration. © *2010 American Institute of Physics*. [doi:10.1063/1.3431011]

I. INTRODUCTION

The liquid-crystalline phase, as a mesophase between the solid and the liquid phase, has been the focus of much research effort because of the fascinating applications of liquid crystals (LCs).[1,2] In addition to conventional LCs, the colloidal suspensions of anisometric particles, such as those composed of colloidal rods and plates, are also able to form liquid-crystalline phase.[3] Similar to LC molecules, anisometric particles may also form long-range orientational and/or positional order, mainly depending on their anisometric shape as well as their concentration. Theoretical consideration on their phase behavior was pioneered by Onsager,[4,5] which was followed by statistical models[6] and numerical simulations.[7,8] Meanwhile, the liquid crystalline phase and the phase transition with the change of particle concentration have been witnessed in a mass of colloidal suspensions composed of anisometric inorganic,[9–12] organic,[13,14] and biological[3,15,16] particles. In most of these suspensions, however, the employed particles were obtained from chemical synthesis, which is time consuming, has low output, and is generally result in broad particle size distribution. This situation has become one of the problems that hinder further investigation on such systems both in theory and in application. Convenient model suspensions are therefore highly desirable.

On the other hand, it is pointed out that the nucleation of nonspherical molecules (e.g., building blocks of LCs) may form crystals that are strongly anisometric.[17,18] This provides a new approach to achieve anisometric particle suspensions. Recent molecular dynamics (MD) simulations[19,20] have shown that the early stage of this nucleation process may result from the aggregation of LC nanodroplets from homogeneous solution. In these simulations, anisometric nanodroplets were observed and the ordering inside the droplet was found to be dependent on temperature and solute concentration for a given solute-solvent interaction. Experimentally, fascinating anisometric droplets, known as tactoids, were also observed in supersaturated suspensions of rodlike particles, for example, the solutions of F-actin[21] in which monodispersed tactoids were obtained at the absence of perturbation. To the best of our knowledge, no experimental observation concerning the nucleation of small nonspherical molecular has been reported. Nonetheless, we believe quench on the solutions of LCs dissolved in appropriate solvents may be expected to obtain anisometric LC microcrystals. Now that LC molecules are identical, the LC microcrystals may also be monodispersed like tactoids. Once anisometric microcrystals are formed, the liquid-crystalline phase formed by the microcrystals and the isotropic-nematic phase transition with increasing microcrystal concentration can be easily expected.

Following this idea, we employed ethanol solutions of 4-cyano-4-n-hexylbiphenyl (6CB) with different 6CB concentrations in this study. By simply quenching these mixture

[a)]Author to whom correspondence should be addressed. Electronic mail: nozaki@dielectrics.sci.hokudai.ac.jp.

solutions, we expect to obtain colloidal suspensions composed of anisometric 6CB microcrystals. We also expect to observe an isotropic to nematic transition in these suspensions with the increase of the concentration of 6CB microcrystal. Instead of polarized microscope, which is the most commonly used method to characterize liquid crystalline phase but is generally not accessible to very low temperatures, we use dielectric spectroscopy (DS) to characterize these mixtures. Because of its high sensitivity to the fluctuation of dipole moments and ionic motions over wide ranges of temperature and pressure, as well as its other advantages such as noninvasion, DS now occupies a special place among numerous modern methods in the characterization of materials.[22] This method is especially suitable for the present system. First, DS is quite mature in the characterization of colloidal suspensions.[23–30] Because the present systems are expected to be colloidal suspensions of microcrystal, DS investigation may provide information on the size, the shape, and the suspension state of the microcrystals. Second, DS is very sensitive to dynamic process, which is generally not easy to be detected by other methods. As aggregate of LC molecules, LC microcrystals may have similar dynamics as LC molecules,[31–38] so investigation on the dielectric behavior may offer information on microcrystal ordering.

It will be shown in this paper that the liquid-crystalline phase composed of 6CB microcrystals can be achieved by quenching 6CB/ethanol mixtures and that the isotropic to nematic phase transition with increasing microcrystal concentration can be confirmed by the dielectric behaviors of the mixtures.

II. EXPERIMENT AND METHODS

A. Materials and preparation of 6CB/ethanol mixtures

The typical LC material, 6CB, was purchased from Sigma-Aldrich and was used without further purification. Ethanol with analytical grade was purchased from Wako Pure Chemical Industries, Japan. The 6CB/ethanol mixtures with different weight fractions of 6CB (18.4%, 15.8%, 13.25%, 10.34%, 6.85%, and 3.55%) were confected by dissolving corresponding amount of 6CB into ethanol, which were shaken and kept for 24 h prior to dielectric and DSC measurements.

B. Dielectric measurement

Dielectric measurements (40 Hz–110 MHz) were carried out with an impedance analyzer (Agilent Technology HP 4294A). The coaxial sample cell, schematically illustrated in Fig. 5.4 in Ref. 39 is composed of an outer conductor with an inner diameter of 3.5 mm and a center conductor with an outer diameter of 2 mm. The lengths of the inner and outer conductor are 10 and 25 mm, respectively. The values of the complex permittivity were obtained from reflection measurements with the sample cell located at the end of a coaxial line. The temperature was controlled by using a Compact Ultra Low Temperature Chamber (MC-811, ESPEC Corp., Japan). The samples held by the sample cell were first quenched from room temperature to −45 °C, at a rate of about 6 °C/min, and then the dielectric measurements were performed at temperature points with an accuracy of ±0.1 °C from −35 to 35 °C with an interval of 5 °C. Except for the mixtures, dielectric measurements were also performed on pure ethanol as reference.

C. Differential scanning calorimetry

The differential scanning calorimetry (DSC) measurement was performed with differential scanning calorimeter (Seiko Instruments DSC6200). Ethanol was used as reference, and the DSC measurement was performed on the 6CB/ethanol mixtures by a quench process from 20 to −50 °C followed by a heating process from −50 to 30 °C. Between the quench process and the heating process, the samples were kept at −50 °C for 10 min for aging. A scanning rate of 6 °C/min was used in both processes, consistent with that in the dielectric measurement.

D. Direct sample observation

The cuvette filled with the 6CB/ethanol mixture was placed in the chamber and subjected to a quench and heating process the same as that in the dielectric measurement. This quench and heating process was observed by direct visual inspection through the window of the chamber and was recorded by means of a digital camera placed in the chamber.

III. RESULTS AND DISCUSSION

A. DSC

Figure 1 shows the DSC curves for the 6CB/ethanol mixtures with different 6CB concentrations during the quench (a) and the subsequent heating process (b). As can be seen in this figure, expect for the 3.55% 6CB mixture, other mixtures show obvious phase transition in both processes. The phase transition is much different from that of bulk 6CB, which has an isotropic-nematic transition at 29 °C and a nematic-crystalline transition at 14.5 °C. In the quench process, the phase transition is strongly dependent on the concentration of 6CB (C_{6CB}), indicated by a decreasing of peak intensity and a downward shifting of transition temperature with decreasing C_{6CB}. This is a typical crystallization process for molecular binary solutions; however, it is also possibly due to the isotropic-nematic phase transition inside the LC droplets, according to the MD simulation.[19,20] In the heating process, the dependence of peak intensity on C_{6CB} is similar to that in the quench process. It is worth noting that the transition temperature for all mixtures keeps nearly constant, namely, it is concentration independent. It is shown that the transition temperature of isotropic-nematic transition inside the LC droplets is strongly dependent on solute concentration.[19] Furthermore, in a similar LC solution composed of 5CB and benzene,[36,37] the bulklike isotropic-nematic phase transition only shows up at high LC concentration range (>70 wt %) and the transition temperature also strongly depends on LC concentration; whereas at low LC concentration range, the crystalline-isotropic phase transition (melting) temperature is almost independent of LC concentration. According to these facts, the concentration

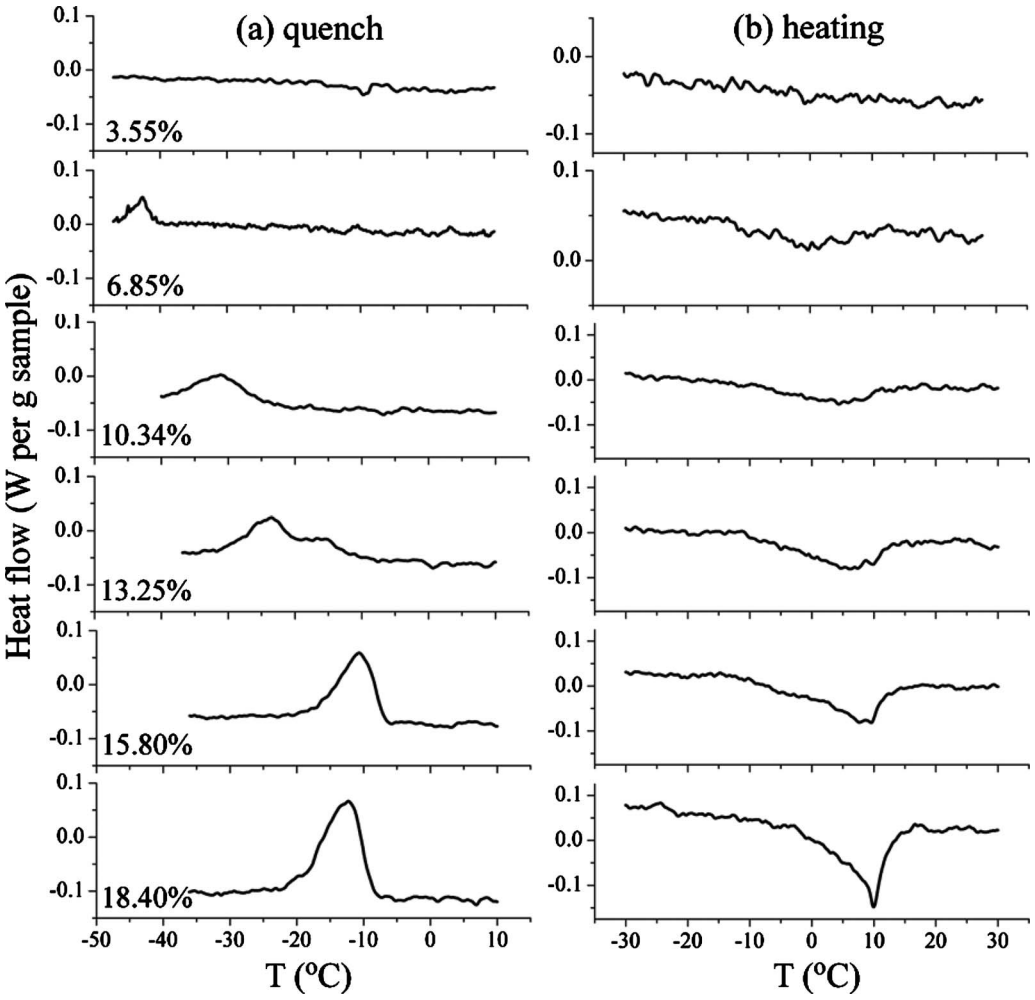

FIG. 1. DSC curves of 6CB/ethanol mixtures with different 6CB concentration during the quench (a) and the subsequent heating (b) processes.

independence of transition temperature shown in Fig. 1(b) definitely indicates that this process is a melting process. Correspondingly, the quench process is a crystallization process. The phase transition inside the LC droplets may occur, but it cannot be resolved from DSC measurement, at least for the present case.

B. Direct observation on the quench and heating processes

The crystallization/melting process can also be observed by direct visual inspection, as shown in Figs. 2 and 3. For the 18.40% 6CB mixture, the crystallization started at about −15 °C and lasted within 1 min, as shown in Fig. 2. Cloud first appeared from the bottom of the cuvette, later from the wall, and then rapidly extended to the whole solution. After about 35 s, the sample did not show obvious change even at much lower temperature. This process looked like the isotropic to nematic phase transition of bulk LCs, and the final state of the whole sample also looked like a nematic phase. We believe the nematiclike phase is composed of fine 6CB crystals. The melting process occurred gradually from the top of the cuvette to the bottom, during which the nematiclike phase at the bottom was quite stable when the temperature was lower than −5 °C. Similar phenomena were also observed for the mixtures with 15.80% and 13.25% 6CB, but the crystallization temperature decreased with decreasing C_{6CB}.

The crystallization of the mixtures with 10.34% and 6.85% 6CB is obviously different from that of the other three mixtures, as shown in Fig. 3. The crystallization process was much slower, and the amount of 6CB crystal increased with decreasing temperature. Not until −35 °C was no macroscopic change observed. Instead of nematiclike, the sample looked translucent and amorphouslike. However, the melting process also started from the top of the sample, and the bottom of the sample did not show any macroscopic change at low temperature range. No crystallization process was observed in the 3.55% 6CB mixture at the temperature range investigated.

A critical concentration seems to exist between 13.25% and 10.34%, higher than which the nucleation is much easier and the crystallization occurs rapidly; otherwise more difficult and much slower. In addition, the macroscopic appearance of the sample is also obviously different between these two groups of mixtures. One has to bear in mind, however, because the crystallization process is very sensitive to environments such as pressure, impurity, and the shape and ma-

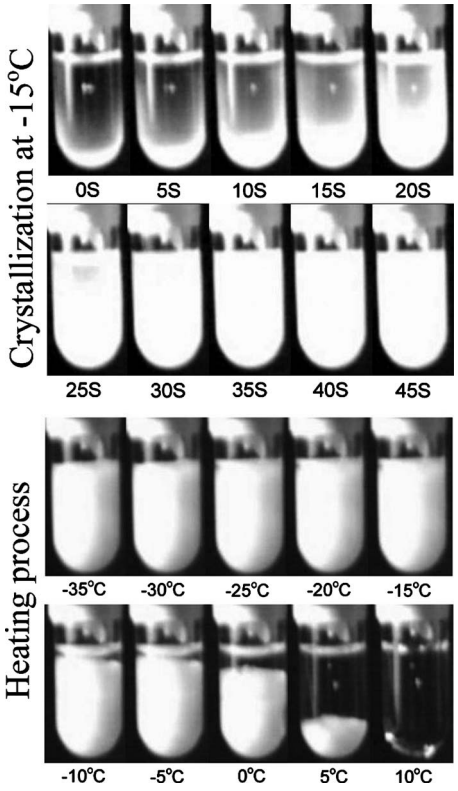

FIG. 2. Direct observation of the crystallization and melting processes of the 6CB/ethanol mixture with 18.4% 6CB.

terials of the container,[40] the actual crystallization process in the dielectric and DSC measurement might be different from what was observed.

C. Dielectric behavior during heating process

Figure 4 shows the temperature and frequency dependences of relative permittivity (a) and dielectric loss (b) of the 18.40% 6CB mixture, from which three regions can be clearly seen: a fluent shifting of dielectric relaxation from −35 to −5 °C (region A), a transition dielectric behavior between −5 and 5 °C (region B), and a region with no dielectric relaxation (region C). Comparing Fig. 4 with Figs. 1 and 2, we can find that region A corresponds to the temperature range where stable crystals exist, region B corresponds to the melting process, and region C corresponds to the temperature range where no crystal exists. Other samples show similar dielectric behaviors. Accordingly, one can easily conclude that the dielectric relaxations are due to the existence of 6CB crystal.

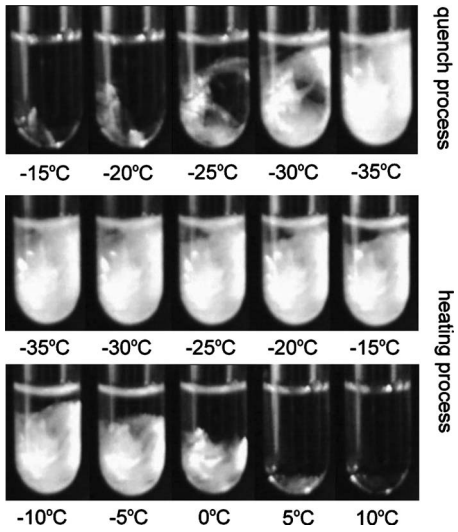

FIG. 3. Direct observation of the crystallization and melting processes of the 6CB/ethanol mixture with 10.34% 6CB.

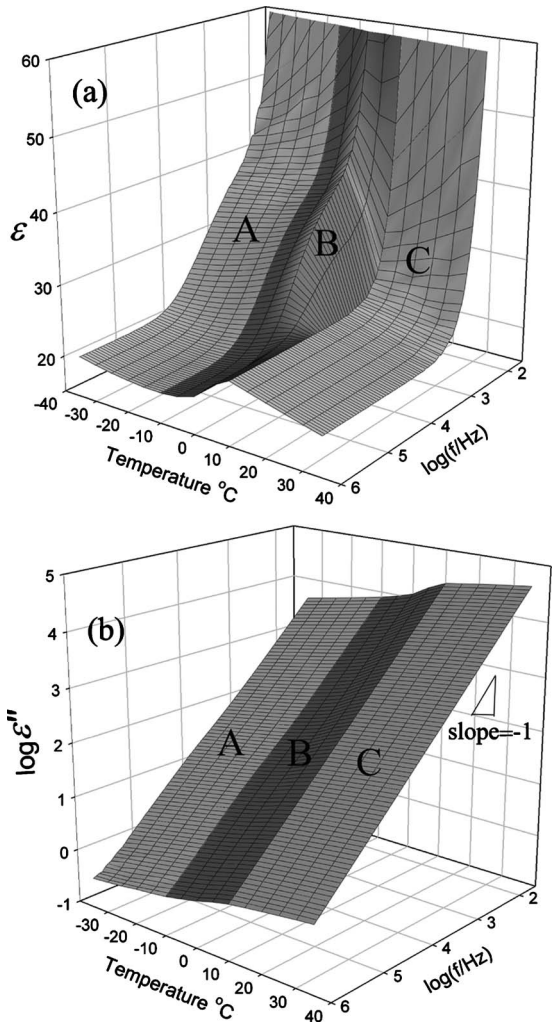

FIG. 4. 3D plots of the real (a) and imaginary (b) part of complex permittivity of the 6CB/ethanol mixture with 18.4% 6CB as functions of temperature and frequency.

D. dc conductivity

It can be seen from Fig. 4(b) that the relaxations are almost totally covered by dc conductivity. The dc conductivity is characterized by the linearity with a slope of minus unity at low frequency range in a $\log \varepsilon'' \sim \log f$ plot.[22] Through the intercepts of the linearity the values of dc conductivity were determined. The dependence of logarithmic dc conductivity on the reciprocal absolute temperature is shown in Fig. 5. For a stable system, its dc conductivity follows Arrhenius law[41] as expressed by

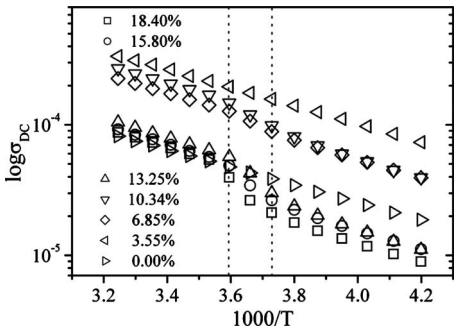

FIG. 5. Arrhenius diagrams of the dc conductivity of ethanol and 6CB/ethanol mixtures with different 6CB concentration.

$$\sigma_{\mathrm{dc}} = \sigma_0 \exp\left(-\frac{E_{\mathrm{dc}}}{k_B T}\right), \tag{1}$$

where σ_0, E_{dc}, k_B, and T are the high temperature limit of conductivity, activation energy, Boltzmann constant, and absolute temperature, respectively. Because no crystallization occurs for the 3.55% 6CB mixture and for ethanol, their temperature dependences show perfect linearity over the whole temperature range. For other samples, different linearity remains both at $T>5$ °C (with smaller slope) where no crystals exist, and at $T<-5$ °C (with larger slope) where stable 6CB crystals exist. This different linearity indicates that the existence of 6CB crystals changes the way of conduction. The good linearity at $T<-5$ °C also suggests that the samples are very stable at this temperature range, even though crystals are present.

When $T>5$ °C, the dc conductivity of ethanol is the lowest; with the addition of 6CB, there is an abrupt increase of σ_{dc} from ethanol to the 3.55% 6CB mixture, then σ_{dc} decreases with increasing $C_{6\mathrm{CB}}$. It is believed that the electrical conductivity of ethanol solution follows a hopping mechanism,[42] proton or other ions transmitting through the chain of ethanol molecules from one electrode to the other. Because LCs cannot be absolutely free from impurity, we believe the abrupt increase of σ_{dc} is due to the introduction of impurity, which increases the concentration of proton or other ions. With increasing $C_{6\mathrm{CB}}$, however, more chainlike structures of ethanol molecules are interfered by 6CB molecules, which consequently slows down the charge transfer and leads to a decreasing σ_{dc}. When $T<-5$ °C, it is noteworthy that the values of σ_{dc} for the 18.40%, 15.80%, and 13.25% 6CB mixtures are even lower than that of ethanol, which implies a further interference in ethanol chains and thus suggests a more complex conformation in these mixtures. The values of the activation energy of all samples at $T<-5$ °C was obtained by fitting the linearity in line with Arrhenius equation, which are listed in Table I.

E. Complex conductivity spectra

Because of dc conductivity, electrode polarization (EP) occurs as a result of the accumulation of space charges on the electrode surface. This notorious effect is very difficult to be eliminated, even though many methods[43,44] have been addressed on it. We tried some of these methods, but none of them is effectively applicable to the present case, maybe because parts of 6CB crystals were nucleated on the surface of the electrodes. Alternatively, we use complex conductivity increment $\Delta\sigma^*$ to characterize the relaxations, which relates with complex permittivity increment $\Delta\varepsilon^*$ by $\Delta\sigma^* = i\omega\varepsilon_0\Delta\varepsilon^*$ (i, $\omega(=2\pi f)$, and ε_0 are imaginary unit, angular frequency, and the permittivity of vacuum, respectively), therefore

$$\Delta\sigma = \sigma - \sigma_{\mathrm{dc}} = \omega\varepsilon_0\Delta\varepsilon'',$$
$$\Delta\sigma'' = \omega\varepsilon_0\Delta\varepsilon = \omega\varepsilon_0(\varepsilon - \varepsilon_\infty), \tag{2}$$

where ε_∞ is the limiting relative permittivity at high frequency, which can be accurately determined from the relative permittivity spectra [Fig. 4(a)]. According to Eq. (2), because EP generally occurs at very low frequency range, the introduction of angular frequency ω into $\Delta\sigma^*$ can enormously decrease the magnitude of EP meanwhile increase the magnitude of relaxations at higher frequency. By using this way the influence of EP can be largely reduced, as clearly shown in Fig. 6 and 7.

TABLE I. Activation energy derived from the Arrhenius plots of dc conductivity and dielectric relaxations at low temperature range, for 6CB/ethanol mixtures with different weight concentration of 6CB and ethanol. The subscripts dc, 1, 2, and 3 denote dc conductivity, relaxation 1, 2, and 3, respectively.

wt %	$E_{\mathrm{dc}}(\pm1\%)$ (kJ/mol)	$E_1(\pm2\%)$ (kJ/mol)	$E_2(\pm2\%)$ (kJ/mol)	$E_3(\pm1\%)$ (kJ/mol)
18.40	14.05	22.51	20.21	14.32
15.80	13.88	22.19	19.42	14.06
13.25	14.53	22.74	20.06	14.14
10.34	13.55	17.91	17.95	13.58
6.85	13.32	17.65	17.04	13.45
3.55	12.87	…	…	…
0.00	12.88	…	…	…

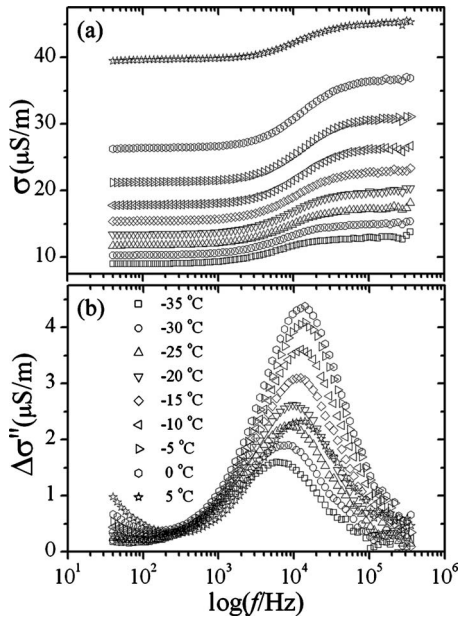

FIG. 6. Imaginary (a) and real (b) part of complex conductivity of the 6CB/ethanol mixture with 18.4% 6CB as a function of frequency at different temperature.

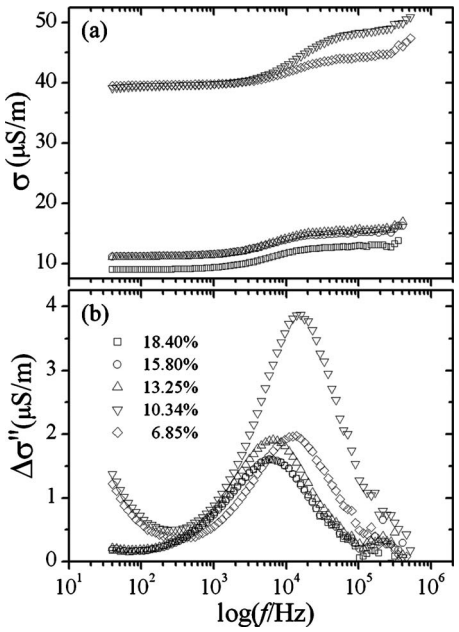

FIG. 7. Imaginary (a) and real (b) part of complex conductivity of 6CB/ethanol mixtures with different 6CB concentration at −35 °C.

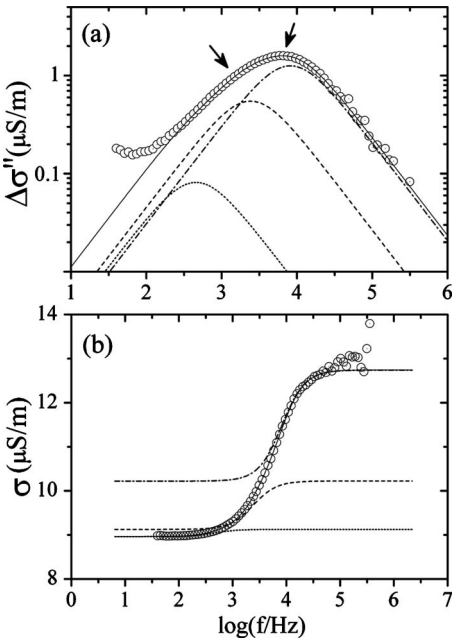

FIG. 8. Example of the fitting result of complex conductivity spectra by means of three terms of Debye function. Short dot: relaxation 1; Short dash: relaxation 2; Short dash dot: relaxation 3; Solid line: the sum of 3 relaxations.

Figure 6 shows the real and imaginary $\Delta\sigma^*$ spectra of the 18.40% 6CB mixture at different temperatures, where the relaxations show a strong dependence on the temperature. Figure 7 shows the $\Delta\sigma^*$ spectra of the mixtures with different C_{6CB} at −35 °C. Very distinctly, the mixtures with $C_{6CB} \geq 13.25\%$ and those with $C_{6CB} \leq 10.34\%$ have different dielectric behaviors. The latter group of mixture has much larger conductivity and higher relaxation frequency. This is consistent with the direct observation, where the crystallization process and the appearance of 6CB crystals are different between the two groups of mixtures. This difference also suggests an essential difference in the phase conformation between these two groups of mixtures.

F. Determination of relaxation parameters

Figure 8 shows one of the fits from complex conductivity increment spectra. The curve of imaginary part of $\Delta\sigma^*$ shown in Fig. 8(a) is strongly asymmetric, and two peaks as indicated by the arrows are distinguishable. In principle, one should fit relaxation curves by using as fewer relaxation terms as possible. Accordingly, we tried to fit the curve by two Havriliak–Negami functions,[45]

$$\sigma^* = i\omega\varepsilon_0\left(\varepsilon_\infty + \sum_i \frac{\Delta\varepsilon_i}{[1+(i\omega\tau_i)^{\alpha_i}]^{\beta_i}}\right), \tag{3}$$

where $\Delta\varepsilon$, ε_∞, and τ are relaxation intensity, high frequency limiting permittivity, and relaxation time, respectively. The parameters α and β describe the shape of the curve, which generally satisfy $0<\alpha\leq 1$ and $0<\beta\leq 1$. Using the double Havriliak–Negami equation, Eq. (3) for the $i=2$ case, we never achieved satisfactory fits when the parameter β was constrained to the range of $0<\beta\leq 1$. This situation indicates that an additional relaxation lies at even lower frequency range, as shown in Fig. 8(a). We then tried to fit the curves by three relaxation terms. Interestingly, we found that the best fitting could be simply achieved by a combination of three Debye functions,

$$\sigma^* = i\omega\varepsilon_0\left(\varepsilon_\infty + \frac{\Delta\varepsilon_1}{1+i\omega\tau_1} + \frac{\Delta\varepsilon_2}{1+i\omega\tau_2} + \frac{\Delta\varepsilon_3}{1+i\omega\tau_3}\right), \tag{4}$$

where the subscripts 1, 2, and 3 represent successive dielectric relaxations from low to high relaxation frequency. By using this fitting function [Eq. (4)], we are trying to characterize the relaxations by the parameters (permittivity) that are familiar to most readers.

The curve fitting was performed by utilizing the software AGILENT VEE PRO 7.0, during which the real and imaginary parts of complex conductivity increment were fit simultaneously to optimize the fitting result. As can be seen in Fig. 8, the three Debye terms fitting function fits well with the experimental curves. To ensure the fitting result more accurate, we have tried different sets of initial variables for the same experimental curves. The results showed that, the relaxation parameters of relaxation 2 and 3 are independent of the initial variables, but those of relaxation 1 are somewhat mutable. This is mainly because relaxation 1 still suffers from EP, especially for the samples with higher dc conductivity. Accordingly, for relaxation 2 and 3, the uncertainty of relaxation intensity and relaxation frequency are generally within 1%, but relaxation 1 is less defined with an uncertainty may up to 5%.

G. Discussion on the mechanisms of the dielectric relaxations

Figure 9 shows the temperature dependence of relaxation frequency ((a), Arrhenius plots) and relaxation intensity $\Delta\varepsilon$ (b), respectively, of the three dielectric relaxations of the mixtures with different C_{6CB}. According to Fig. 9(a), the re-

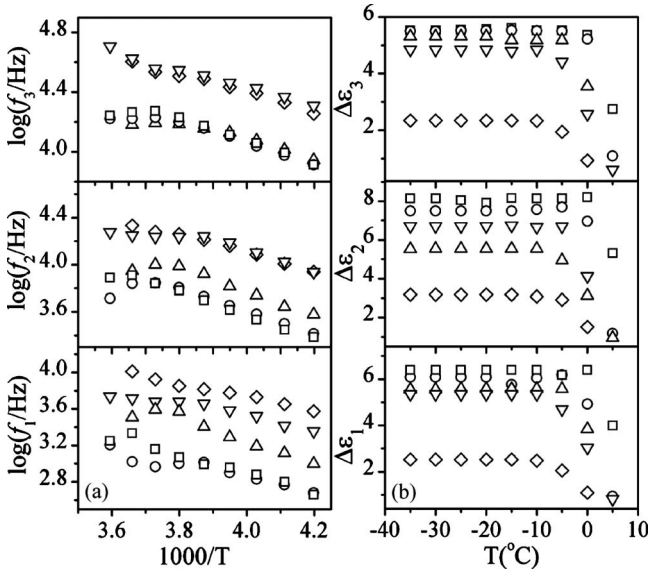

FIG. 9. Temperature dependence of the relaxation frequency (a) and the relaxation intensity (b) of relaxation 1, 2, and 3 for 6CB/ethanol mixtures with different 6CB concentration. □ 18.40%, ○ 15.80%, △ 13.25%, ▽ 10.34%, and ◇ 6.85%.

laxation frequency of all relaxations follows well with Arrhenius manner when $T<-5$ °C, once more indicating that the crystals are stable at low temperature. The relaxation frequency does not change so regularly at the transition temperature range between −5 and 5 °C. This irregularity is mainly because of the melting of 6CB crystals at this temperature range. The activation energy of each dielectric relaxation at low temperature range ($T<-5$ °C) was derived by fitting the Arrhenius diagrams by means of the Arrhenius dependence

$$\log f_i = \log f_0 + \frac{E_i}{2.303RT}, \tag{5}$$

where R and the subscript i represent the gas constant and the ith dielectric relaxation, respectively. The values of these activation energies are also listed in Table I, from which we notice that E_3 is always equivalent to E_{dc} for all mixtures. This means relaxation 3 correlates closely with dc conductivity, i.e., this relaxation is possibly ascribed to ionic motion. On the other hand, both E_1 and E_2 are systematically larger than E_{dc}, suggesting that other mechanism rather than ionic motion is accounting for these relaxations.

Considering that the present mixtures at low temperature are colloidal suspensions of 6CB crystals and that a lot of 6CB molecules still exist in the bulk ethanol solution, all the following mechanisms are possibly giving rise to the observed dielectric relaxations: the rotation of 6CB molecules in the bulk solution or in the crystalline phase, the polarization of 6CB crystals, the Maxwell–Wagner (MW) polarization, and the reorientation of 6CB crystals.

H. Rotation of 6CB molecules

Besides extensive investigations on the dielectric properties of bulk alkylcyanobiphenyls,[31–37] the dielectric properties of their mixtures with organic solvent were also investigated.[36,37] The recent study[36] showed that even at low weight fraction of 5CB (30%), apparent dielectric relaxation due to the rotation of 5CB molecules in the bulk solution still showed up for 5CB/benzene mixture. In the present case, the highest weight fraction of 6CB is 18.40%, thus the rotation of 6CB molecules in the bulk solution cannot give rise to such high $\Delta\varepsilon$ [mostly bigger than 5, see Fig. 9(b)], not to mention that this MD generally occurs at a much higher frequency range. On the other hand, although crystallized 6CB molecules in the crystalline phase can also give rise to dielectric relaxation, the relaxation intensity is generally several decimals even for pure LC,[36,37] which is far smaller than that in the present case. Accordingly, the mechanism due to the rotation of 6CB molecules in the bulk solution or in the crystalline phase can be ruled out.

I. Particle polarization and MW polarization

Colloidal suspensions generally exhibit two typical mechanisms of dielectric relaxations, namely, the polarization of suspended particles[25–30] and the MW polarization.[22–24] From the viewpoint of electrodynamics,[26,29] both of the relaxations are ascribed to the field induced dipole moments that arise from charge migration. Therefore, the activation energies of both relaxations should be comparable to that of dc conductivity. Only relaxation 3 is possibly due to either of these mechanisms, judged by the values of its activation energy shown in Table I. In addition, comparing Fig. 5 with Fig. 9(a), we can find that $f_3(=1/2\pi\tau_3)$ follows a similar Arrhenius manner to that of σ_{dc}, which means f_3 is mainly a function of the electrical conductivity (ionic concentration) instead of 6CB concentration.

The relaxation time of particle polarization corresponds to the time for counterions to migrate over a distance of the order of $a+\kappa^{-1}$ for a spherical particle, it thus is estimated by[27]

$$\tau_C = \frac{1}{2\pi f_C} = \frac{4(a+\kappa^{-1})^2}{D_C}, \tag{6}$$

where D_C is the counterion diffusion coefficient and a is the radius of a spherical particle or the half-length of a rod-shaped particle. κ^{-1} denotes the Debye length, which can be estimated from the following equation for 1–1 type electrolyte,

$$\kappa^{-1} = \sqrt{\frac{\varepsilon_m \varepsilon_0 k_B T}{2nq^2}}, \tag{7}$$

where n is the ionic concentration, ε_m is the dielectric constant of solvent, and q is electron charge, respectively. Because the dielectric constant of ethanol barely changes with slight change of ionic concentration, the Debye length is only a function of ionic concentration. As mentioned above, f_3 (τ_3) is only a function of ionic concentration. Therefore, if this mechanism is responsible for relaxation 3, a should be far smaller than κ^{-1} so that a can be neglected from Eq. (6). This is not likely considering that the Debye length is generally on the scale of several nanometers.

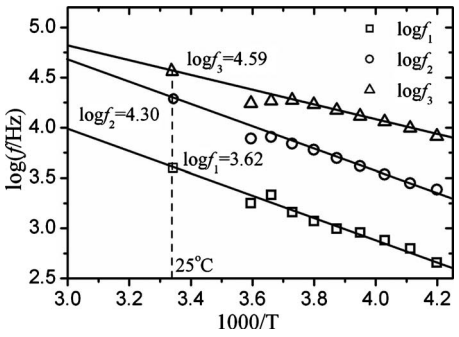

FIG. 10. The extrapolating relaxation frequency of relaxation 1, 2, and 3 at room temperature for the 6CB/ethanol mixture with 18.40% 6CB.

On the other hand, the relaxation time of the MW polarization for a heterogeneous system with two phases can be estimated by[23,24]

$$\tau_{\mathrm{MW}} = \frac{1}{2\pi f_{\mathrm{MW}}} = \frac{2\varepsilon_0(\varepsilon_p + \varepsilon_m)}{4\pi(2\sigma_p + \sigma_m)}, \tag{8}$$

where the subscripts p and m represent the suspended particle and the suspending medium, respectively. In the present case, 6CB crystal is the suspended particle and ethanol solution is the suspending medium. At room temperature, the static dielectric constant of 6CB is about 10 and that of ethanol solution is about 24. The conductivity of the ethanol solution (σ_m) of the mixtures at room temperature can be determined by extrapolating the Arrhenius manner of dc conductivity in Fig. 5, which is of the order of $O10^{-5}$–$O10^{-4}$ S/m. Compared to σ_m, σ_p is so small that it can be neglected from Eq. (8); therefore, this equation can be simplified as

$$\tau_{\mathrm{MW}} = \frac{1}{2\pi f_{\mathrm{MW}}} = \frac{2\varepsilon_0(\varepsilon_p + \varepsilon_m)}{4\pi\sigma_m}. \tag{9}$$

According to this equation, $\tau_{\mathrm{MW}}(f_{\mathrm{MW}})$ is only a function of σ_m, considering that ε_p and ε_m keep almost constant for all mixtures. Estimated from Eq. (9), the relaxation frequency of the MW polarization at room temperature is of the order of $O10^5$ for the 18.40% 6CB mixture. Figure 10 shows the Arrhenius diagram of the relaxation frequency of the three dielectric relaxations of the 18.40% 6CB mixture, by which the relaxation frequency at room temperature can be determined by extrapolating the Arrhenius manner. As clearly shown in Fig. 10, the extrapolated relaxation frequency of relaxation 3 is consistent with what estimated from Eq. (9). These facts definitely indicate that relaxation 3 is originated from the MW polarization.

J. Reorientation of 6CB microcrystals

As pointed out above, 6CB microcrystals are supposed to be anisometric, which may possess a shape similar to 6CB molecule. More importantly, as highly ordered aggregates of 6CB molecules that possess permanent dipole moment, 6CB microcrystals also possess strong dipole moment. Therefore, it is reasonable to believe that 6CB microcrystals have similar orientational dynamics as that of single 6CB molecule.[22,31–38] Similarly, we can suppose that each 6CB microcrystal has a longitudinal $\mathbf{P}_l$ and a transversal $\mathbf{P}_t$ permanent dipole moment, and at least two relaxation modes can be realized [schematically shown in Fig. 11(a)]. The rotation of $\mathbf{P}_t$ around the long axis (mode 1) and the reorientation of $\mathbf{P}_l$ (mode 2). The former mode has a smaller relaxation time because of the smaller moments of inertia involved; and the latter one is associated with the small changes of the angle between $\mathbf{P}_l$ and the director $\mathbf{n}$ (Refs. 22 and 38) instead of an end-over-end rotation. Judging from Fig. 9, we can ascribe relaxation 2 to mode 1 and relaxation 1 to mode 2.

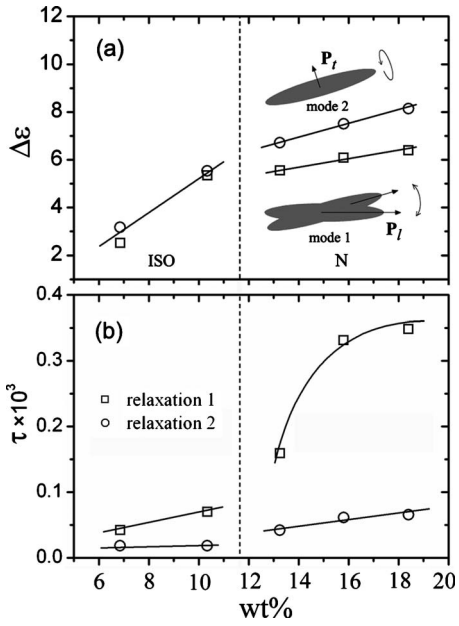

FIG. 11. Relaxation intensity (a) and relaxation time (b) of relaxation 1 (open square) and relaxation 2 (open circle) at −35 °C, as a function of the weight fraction of 6CB. The lines were drawn for guiding the eyes, and the relaxation modes are also schematically presented.

The relaxation time of orientational rotation can be roughly estimated from the following equation:

$$\tau = \frac{4\pi\eta a^3}{k_B T}, \tag{10}$$

where η is the viscosity of bulk solution, and other symbols have the same meaning as mentioned above. At room temperature, the viscosity of ethanol is about 1.07×10^{-3} Pa s. Through the extrapolated relaxation frequency of relaxation 1 and 2 in Fig. 10, the half-length of the long and short axes of the 6CB microcrystal can be estimated in line with Eq. (10), which are 22.9 nm and 13.5 nm, respectively, for the mixture with 18.40% 6CB. Although it is a rough estimation, these values remain in a reasonable range and the aspect ratio ($\approx$1.7) of the 6CB microcrystal is approximate to what observed in MD simulation.[19,20]

K. The phase transition with the change of 6CB concentration

As previously mentioned, the suspensions of anisometric particle can form liquid crystalline phase when the particle concentration attains to a sufficiently high value. This phenomenon was first interpreted theoretically by Onsager,[4,5]

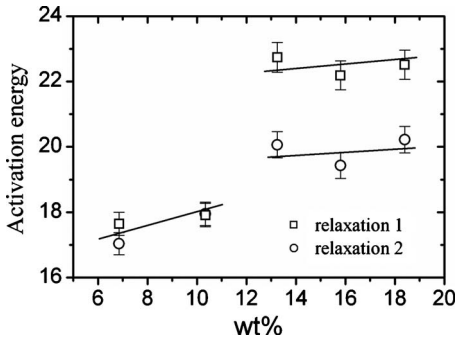

FIG. 12. Activation energy of relaxation 1 (open square) and relaxation 2 (open circle) as a function of the weight fraction of 6CB.

who indicated that the stability of the nematic phase of rodlike particle suspensions lies in the competition between the orientational entropy (in favor of isotropic state) and the excluded volume entropy (which favors nematic state). When the particle concentration is sufficiently high, the excluded volume entropy becomes more important, a first order phase transition from isotropic to nematic phase may occur. This notion has been confirmed by many computer simulations[7,8] and experimental investigations.[9–15] In the present case, because the suspended particles (6CB microcrystals) are supposed to be anisometric, such kind of phase transition with the change of particle concentration may also exist.

It can be noted from Fig. 5 that the dc conductivity of the mixtures with $C_{6CB} \geq 13.25\%$ is even smaller than that of pure ethanol at $T < -5$ °C, which implies that a quite compact conformation presents in these mixtures. Additionally, when temperature decreases from the high temperature region (>5 °C) to the low temperature region (<−5 °C), the dc conductivity of the mixtures with $C_{6CB} \geq 13.25\%$ decreases more obviously than those with $C_{6CB} \leq 10.34\%$, which also indicates an essential change in the conformation between these two groups of mixtures. Figure 12 shows the dependence of the activation energy of relaxation 1 and 2 on C_{6CB}, from which it can be seen that remarkable increase shows up when $C_{6CB} \geq 13.25\%$. This means that the rotation/reorientation of the 6CB microcrystals in the mixtures with higher C_{6CB} are much more restricted. Although particle interaction increases with increasing particle concentration, which may also restrict the rotation/reorientation of the particle, we believe this effect cannot give rise to such remarkable increase in activation energy. It is thus most likely that the 6CB microcrystals in the mixtures with higher C_{6CB} are aligned orderly. According to these behaviors, we can argue that: when $C_{6CB} \geq 13.25\%$, the microcrystals are orientationally ordered and a nematic phase exists. Under this condition, the excluded volume entropy dominates because of the high concentration of 6CB microcrystals; whereas when $C_{6CB} \leq 10.34\%$, the orientational entropy dominates and the 6CB microcrystals are in an isotropic state. This scenario also explains the different appearance of these two groups of mixtures (Figs. 2 and 3). The nematiclike phase in the mixtures with $C_{6CB} \geq 13.25\%$ is composed of ordered 6CB microcrystals, while the 6CB microcrystals in the amorphouslike phase in the mixtures with lower C_{6CB} are disordered.

The variations of the relaxation parameters for relaxation 1 and relaxation 2 also indicate this isotropic-nematic phase transition, as displayed in Fig. 11, where the relaxation intensity $\Delta\varepsilon$ and the relaxation time τ at −35 °C are plotted as a function of C_{6CB}. From Fig. 11(a) we can see that $\Delta\varepsilon$ basically increases as C_{6CB} increases, this is because the concentration of 6CB microcrystal increases with increasing C_{6CB}. Due to the excluded volume effect, the reorientation around the short axis (mode 2) is much more restricted and therefore has a smaller rotation angle at nematic phase than at isotropic phase. On the other hand, because mode 1 has much smaller excluded volume effect than mode 2,[36] the excluded volume effect is much less effective to the rotation around the long axis. As a result, $\Delta\varepsilon_1$ is noticeably smaller than $\Delta\varepsilon_2$ at nematic phase, but they are very close to each other at isotropic phase. For relaxation 1, an abrupt increase of τ_1 can be seen from Fig. 11(b) between isotropic and nematic phase. This is because, the 6CB microcrystals can freely rotate around their short axis at isotropic phase, but the rotation is much more restricted at nematic phase due to the ordering of 6CB microcrystals. The increase of τ_2 is not so profound, because the rotation around long axis is not so restricted by the small excluded volume effect. The variations of $\Delta\varepsilon$ and τ of relaxation 1 and relaxation 2 in turn prove that mode 1 and mode 2 are responsible for the relaxation 2 and relaxation 1, respectively.

IV. CONCLUDING REMARKS

The suspensions of 6CB microcrystal dispersed in ethanol were obtained by simply quenching 6CB/ethanol mixtures, and nematiclike phase can be directly observed for the mixtures with higher 6CB concentration. After quench, dielectric measurements were carried out on the mixtures at increasing temperature points. It was found from the dielectric spectra that there are three obvious dielectric behavior regions, which correspond to three temperature regions, namely, the higher temperature region (>5 °C) where no crystals exist, the intermediate temperature region (between −5 and 5 °C) where a lot of crystals has been melt, and the lower temperature region (<−5 °C) where stable crystals exist, respectively.

For the temperature regions where crystals present, three overlapping dielectric relaxations were observed at the frequency range between 10^3 and 10^5 Hz, which were perfectly characterized by a combination of three Debye functions. The relaxation parameters derived from curve fitting, including relaxation frequency and relaxation intensity, showed strong dependence on temperature and C_{6CB}. It is concluded that the relaxation with the highest relaxation frequency is due to the MW polarization, and the relaxations with lower relaxation frequency are due to the rotation/reorientation of the 6CB microcrystals around the long and short axis, respectively. It is also concluded from the dielectric behaviors that, when $C_{6CB} \leq 10.34\%$, 6CB microcrystals are in an isotropic state; whereas when $C_{6CB} \geq 13.25\%$, nematic phase composed of 6CB microcrystals appears.

Because all dielectric relaxations are of Debye type, the 6CB microcrystals are believed to be monodispersed in the ethanol solution, the present system thus is hoped to become

a model system both in the fundamental research on the liquid-crystalline properties of anisometric colloidal suspensions and in searching for new applications of LCs. It is also demonstrated that DS is effective to characterize the phase composition and the phase transition of anisometric particle suspensions.

ACKNOWLEDGMENTS

This work is partly supported by KAKENHI (Grant No. 19340116), Grant-in-Aid for Scientific Research (B), from the Ministry of Education, Culture, Sports, Science and Technology (MEXT) of Japan.

[1] S. Chandrasekhar, *Liquid Crystals* (Cambridge University Press, Cambridge, 1992).
[2] P. J. Collings and J. S. Patel, *Handbook of Liquid Crystal Research* (Oxford University Press, New York, 1997).
[3] F. C. Bawden, N. W. Pirie, J. D. Bernal, and I. Fankuchen, Nature (London) **138**, 1051 (1936).
[4] L. Onsager, Phys. Rev. **62**, 558 (1942).
[5] L. Onsager, Ann. N.Y. Acad. Sci. **51**, 627 (1949).
[6] G. J. Vroege and H. N. W. Lekkerkerker, Rep. Prog. Phys. **55**, 1241 (1992).
[7] J. A. C. Veerman and D. Frenkel, Phys. Rev. A **45**, 5632 (1992).
[8] P. Bolhuis and D. Frenkel, J. Chem. Phys. **106**, 666 (1997).
[9] K. Kajiwara, N. Donkai, Y. Hiragi, and H. Inagaki, Macromol. Chem. Phys. **187**, 2883 (1986).
[10] O. Pelletier, P. Davidson, C. Bourgaux, and J. Livage, Europhys. Lett. **48**, 53 (1999).
[11] H. Maeda and Y. Maeda, Phys. Rev. Lett. **90**, 018303 (2003).
[12] B. J. Lemaire, P. Davidson, D. Petermann, P. Panine, I. Dozov, D. Stoenescu, and J. P. Jolivet, Eur. Phys. J. E **13**, 309 (2004).
[13] X. M. Dong, T. Kimura, J. F. Revol, and D. G. Gray, Langmuir **12**, 2076 (1996).
[14] M. M. D. de Souza Lima and R. Borsali, Macromol. Rapid Commun. **25**, 771 (2004).
[15] Z. Dogic and S. Fraden, Phys. Rev. Lett. **78**, 2417 (1997).
[16] K. R. Purdy, S. Varga, A. Galindo, G. Jackson, and S. Fraden, Phys. Rev. Lett. **94**, 057801 (2005).
[17] A. Donev, I. Cisse, D. Sachs, E. A. Variano, F. H. Stillinger, R. Connelly, S. Torquato, and P. M. Chaikin, Science **303**, 990 (2004).
[18] T. Schilling and D. Frenkel, Comput. Phys. Commun. **169**, 117 (2005).
[19] R. Berardi, A. Costantini, L. Muccioli, S. Orlandi, and C. Zannoni, J. Chem. Phys. **126**, 044905 (2007).
[20] W. M. Brown, M. K. Petersen, S. J. Plimpton, and G. S. Grest, J. Chem. Phys. **130**, 044901 (2009).
[21] P. Oakes, J. Viamontes, and J. X. Tang, Phys. Rev. E **75**, 061902 (2007).
[22] F. Kremer and A. Schonhals, *Broadband Dielectric Spectroscopy* (Springer-Verlag, Berlin, 2002).
[23] J. C. Maxwell, *A Treatise on Electricity and Magnetism*, 3rd ed. (Clarendon, Oxford, 1891).
[24] K. W. Wagner, Archiv für Elektrotechnik **2**, 371 (1914).
[25] G. Schwarz, J. Phys. Chem. **66**, 2636 (1962); J. M. Schurr, *ibid.* **68**, 2407 (1964).
[26] S. S. Dukhin and V. N. Shilov, *Dielectric Phenomena and the Double Layer in Disperse Systems and Polyelectrolytes* (Wiley, New York, 1974).
[27] E. H. B. DeLacey and L. R. White, J. Chem. Soc., Faraday Trans. 2 **77**, 2007 (1981).
[28] W. C. Chew and P. N. Sen, J. Chem. Phys. **77**, 4683 (1982).
[29] R. W. O'Brien, Adv. Colloid Interface Sci. **16**, 281 (1982).
[30] M. L. Jiménez, F. J. Arroyo, J. van Turnhout, and A. V. Delgado, J. Colloid Interface Sci. **249**, 327 (2002).
[31] P. G. Cummins, D. A. Danmur, and D. A. Laidler, Mol. Cryst. Liq. Cryst. **30**, 109 (1975).
[32] J. M. Wacrenier, C. Druon, and D. Lippens, Mol. Phys. **43**, 97 (1981).
[33] H. G. Kreul, S. Urban, and A. Wurflinger, Phys. Rev. A **45**, 8624 (1992).
[34] R. Nozaki, T. K. Bose, and S. Yagihara, Phys. Rev. A **46**, 7733 (1992).
[35] J. Thoen and T. K. Bose, in *Handbook of Low and High Dielectric Constant Materials and Their Applications*, edited by H. S. Nalwa (Academic Press, San Diego, 1999), Vol. 1, pp. 501–561.
[36] S. K. Kundu, S. Okudaira, M. Kosuge, N. Shinyashiki, and S. Yagihara, J. Chem. Phys. **129**, 164509 (2008).
[37] S. K. Kundu, S. Okudaira, M. Kosuge, N. Shinyashiki, and S. Yagihara, J. Phys. Chem. B **113**, 11109 (2009).
[38] Y. Lin, "Dielectric relaxation and electrooptical effects in nematic liquid crystals," Ph.D. thesis, Kent State University, 2007.
[39] T. K. Bose, R. Chahine, and R. Nozaki, in *Microwave Aquametry*, edited by A. Kraszewski (IEEE, New York, 1996), pp. 81–92.
[40] R. P. Sear, J. Phys.: Condens. Matter **19**, 033101 (2007).
[41] A. Catenaccio, Y. Daruich, and C. Magallanes, Chem. Phys. Lett. **367**, 669 (2003).
[42] E. Gileadi and E. Kirowa-Eisner, Electrochim. Acta **51**, 6003 (2006).
[43] F. Bordi, C. Cametti, and R. H. Colby, J. Phys.: Condens. Matter **16**, R1423 (2004).
[44] U. Kaatze and Y. Feldman, Meas. Sci. Technol. **17**, R17 (2006).
[45] S. Havriliak and S. Negami, Polymer **8**, 161 (1967).